

# Longitudinal Forces on a Spherical Dielectric Particle Exerted by a Truncated Bessel Beam in the Ray Optics Regime

Pedro Paulo Justino da Silva Arantes, Leonardo André Ambrosio

Department of Electrical and Computer Engineering (SEL)

São Carlos School of Engineering (EESC), University of São Paulo (USP),  
400 Trabalhador São-carlense Ave., 13566-590 São Carlos, Brazil.

pedro.arantes@usp.br

**Abstract**—A first theoretical and numerical treatment of longitudinal forces in an extended geometrical optics model exerted by a truncated Bessel beam (TBB) on a spherical dielectric particle is presented in this work. To describe the TBB, we use a method for spatial beam shaping to describe truncated beams with simplicity and total analyticity in the paraxial approximation, which utilizes a discrete superposition of scalar Bessel Gauss beams. We present numerical examples of longitudinal forces that a TBB exerts on a scatterer and argue about the limitations of this method. We also briefly discuss about further possible analysis that can be done with TBB and other truncated beams.

**Keywords**— Lasers. Optical beams. Optical diffraction. Electromagnetic forces. Geometrical optics.

## I. INTRODUCTION

Since the first experiments performed by A. Ashkin and others involving the use of lasers for trapping biological particles [1], [2], optical tweezers have been the subject of intensive studies and applications [3]–[10]. Due to its non-invasive features, it has been used in non-contact and non-damage applications, in particular at biomedical optics field, such as manipulation of bacterias and viruses [7], induced cell fusion [11], microscopic observation of living cells [8], [12], chromosome movement [13], DNA insertion in a single cell among others [14], [15]. Besides biology, there are applications in physics and chemistry's branches, like support on macromolecular interactions analysis in colloidal solutions [16], [17] or studies on the vibration dynamics and fluctuations of microtubules field [18]. More recently, optical tweezers served as a valuable tool in evidenciating violations to the Second Law of Thermodynamics over extremely short time intervals [19].

Most published reports about optical tweezers found on the literature use a Gaussian beam (GB) for its analysis. Other that is commonly found is a Bessel Beam (BB) [20]–[22] because of its self-reconstructing and non diffractive properties [23], [24]. However, as far as we know, these works consider

This work was developed from FAPESP resources (project no. 2014/04867-1) and was supported by CAPES (masters scholarship of Pedro Paulo Justino da Silva Arantes).

978-1-5090-6241-6/17/\$31.00 ©2017 IEEE

the BBs as ideal ones, that is, they differ from a real beam in respect to its opening aperture radius. The former has an infinite radius, which means that it receives an infinite amount of energy from its source and, therefore, propagates indefinitely; the latter has a finite opening radius, finite energy and propagates up to a maximum distance  $Z_{max}$ . Real BB is also called truncated Bessel beam (TBB).

Studies with real beams, until now, fall back on the resolution of diffraction's integrals, like Rayleigh-Sommerfeld formula [25, Chap 4], in order to represent a finite-aperture beam. Nevertheless, there are cases in which these integrals do not provide an analytical expression and a BB is one of them. To overcome this problem, we use a method for spatial beam shaping developed by Zamboni-Rached et al. [26], which describes truncated beams with simplicity and total analyticity in the paraxial approximation, utilizing a discrete superposition of scalar Bessel Gauss beams.

Due to the relevance of optical trapping systems and its applications aiming to bringing theoretical descriptions into closer contact with actual laser beams found in the laboratory, the purpose of the present work is to perform theoretical and numerical analysis of optical forces exerted on dielectric particles by real, finite energy scalar BBs, whose fields can be described analytically [26]. To the best of the authors' knowledge, this is the first attempt towards the incorporation of truncated beams in optical force calculations in the ray optics regime. The authors had already done some work with optical force calculation for TBB in the Rayleigh approximation [27].

Firstly, in this work, we revised how TBBs can be described using the method commented above, eliminating the diffraction's integrals' need. Afterward, we study how to calculate optical forces in dielectric spherical particles using TBBs in the paraxial approximation. We also assume the particle radius to be much greater than the wavelength of the incident wave, thus focusing on the geometrical optics regime. Subsequently, numerical results and examples are presented, followed by our conclusions.

## II. THEORY

### A. Truncated Bessel Beam

A scalar TBB in the paraxial regime can be represented by a superposition of distinct Bessel-Gauss beams (BGBs) [26]. A BGB is defined, at the  $z = 0$  plane, as a BB apodized by a Gaussian function, whose propagation is taken along  $+z$  [28]:

$$\psi_{BG}(\rho, z = 0) = AJ_0(k_\rho \rho) e^{-q\rho^2}, \quad (1)$$

where  $A$  is the intensity of the incident field;  $J_0$  zeroth-order Bessel function of the first kind;  $k_\rho$  transverse wave number of the propagating wave and  $q$  a Gaussian function parameter. The temporal factor  $\exp(-i\omega t)$  is omitted for simplicity. As much as the paraxial regime is sub-intended, our analysis is therefore limited to small axicon angles [23].

To represent a BGB over all coordinates, we apply  $\psi_{BG}(\rho, z = 0)$  on Fresnel diffraction integral [25], whose final results is [26]:

$$\psi_{BG}(\rho, z) = -\frac{ikA}{2zQ} e^{ik(z+\frac{\rho^2}{2z})} J_0\left(\frac{ikk_\rho \rho}{2zQ}\right) \times e^{-\frac{1}{4Q}\left(k_\rho^2 + \frac{k^2 \rho^2}{z^2}\right)}, \quad (2)$$

where  $Q = q - ik/2z$  and  $k$  is the wave number.

The proposed solution to represent truncated beams analytically uses a discrete superposition of  $2N + 1$  equal-frequency BGBs. Thus, we have:

$$\Psi(\rho, z) = -\frac{ik}{2z} e^{ik(z+\frac{\rho^2}{2z})} \sum_{n=-N}^N \frac{A_n}{Q_n} J_0\left(\frac{ikk_\rho \rho}{2zQ_n}\right) \times e^{-\frac{1}{4Q_n}\left(k_\rho^2 + \frac{k^2 \rho^2}{z^2}\right)}, \quad (3)$$

in which  $A_n$  are a complex constant and  $Q_n = q_n - ik/2z$ .  $q_n$  is defined by  $q_n = q_r - i2\pi n/L$ , in which  $q_r > 0$  is the real part of  $q_n$  and  $L$  is a constant with dimensions of length squared.  $A_n$  is given by [26]

$$A_n = \frac{2 \sinh \left[ (q_R - q - i\frac{2\pi}{L} n) R^2 \right]}{L(q_R - q) - i2\pi n}. \quad (4)$$

Heretofore, the variables that must be determined are  $L$  and  $q_r$ . Once we have defined  $q$  from (1) and  $A_n$  from (4),  $L$  and  $q_r$  must satisfy the following condition:

$$e^{-q_r \rho^2} \sum_{n=-\infty}^{\infty} A_n e^{i2\pi n \rho^2/L} \approx \begin{cases} e^{-q \rho^2}, & \text{if } 0 \leq \rho \leq R \\ 0, & \text{if } R < \rho < \infty. \end{cases} \quad (5)$$

It is possible to represent other truncated beams by requiring  $q$  and  $k_\rho$  to obey the following conditions [see Eq. (1)]:

- Truncated plane wave (TPW): when  $q$  and  $k_\rho$  are zero;
- TBB: when  $q = 0$  and  $k_\rho$  is its transverse wave number;
- truncated Gaussian beam (TGB): when  $k_\rho = 0$  and  $q = 1/\omega_0^2$ , in which  $\omega_0$  is the desired TGB beam waist;
- truncated Bessel-Gaussian beam (TBGB): when  $k_\rho$  is the BGB transverse wave number and  $q = 1/\omega_0^2$ , in which  $\omega_0$  is the desired BGB beam waist.

### B. Ray Optics Forces on Spherical Particles

Consider a laser beam, whose aperture is parallel to the  $xy$  plane and with center at  $C_a = (x_0, y_0, z_0)$ . It illuminates a spherical dielectric particle fixed at the origin of the coordinate system  $O = (0, 0, 0)$  with radius  $R_p$  and refractive index  $n_p$ . The host medium is water, whose refractive index is 1.33.

It is well-known that light carries momentum [29] which can be transferred to objects. When a light ray hits a bead, there is linear momentum transfer between them, with the consequence that the former will exert an optical force on the latter. To illustrate this, Fig. 1 shows a single ray  $p_i$ , whose direction is  $\hat{k}_0$ , with power density  $dP_i$  impacting on a spherical particle surface at point  $A$  whose normal is  $\hat{n}_0$ . The multiple rays reflected and refracted at the surface of the scatterer are labeled according to its power density. We denote by  $T$  and  $R$  the transmissivity and reflectivity Fresnel coefficients, respectively, at medium-particle interface, and by  $\theta_i$  and  $\theta_r$  the angles of incidence and refraction.

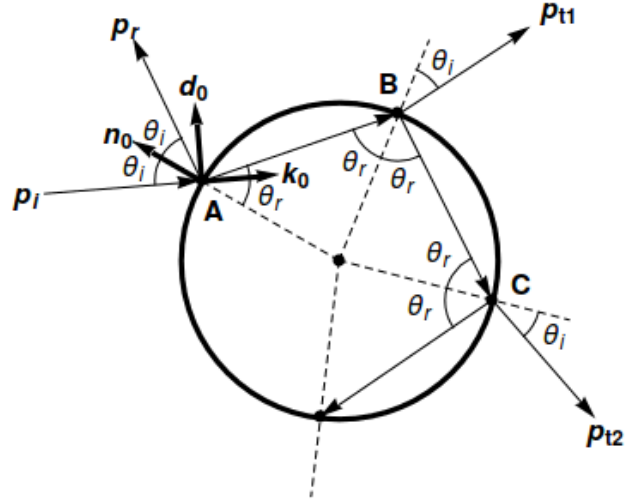


Fig. 1: Schematic diagram of the propagation of a light ray in a dielectric spherical particle.

It can be shown that the radiation pressure  $d\vec{F}$  exerted by  $p_i$ , firstly calculated by Roosen [30] and Ashkin [9], is given by [31]:

$$d\vec{F} = \frac{n_m}{c} [\text{Re}(Q_t) \hat{k}_0 + \text{Im}(Q_t) \hat{d}_0] dP_i, \quad (6)$$

where  $\hat{k}_0$  is given by the phase gradient of  $\Psi$  and  $\hat{d}_0$  is the orthonormal vector with respect to  $\hat{k}_0$ , given by:

$$\hat{d}_0 = \frac{\hat{n}_0 - (\hat{n}_0 \cdot \hat{k}_0) \hat{k}_0}{|\hat{n}_0 - (\hat{n}_0 \cdot \hat{k}_0) \hat{k}_0|}, \quad (7)$$

and  $Q_t$  by [32]:

$$Q_t = 1 + Re^{-i2\theta_i} - T^2 \frac{e^{-i2(\theta_i - \theta_r)}}{1 + Re^{i2\theta_r}}. \quad (8)$$

The transmissivity and reflectivity can be written as [33, Chap 1]:

$$R(\theta_i, \theta_r) = \frac{\sin^2(\theta_i - \theta_r)}{\sin^2(\theta_i + \theta_r)} \sin^2 \beta + \frac{\tan^2(\theta_i - \theta_r)}{\tan^2(\theta_i + \theta_r)} \cos^2 \beta, \quad (9)$$

in which  $\beta$  is the crossing angle between the electric field direction and the normal to the plane of incidence (plane in which  $\hat{k}_0, \hat{d}_0$  and  $\hat{n}_0$  are contained [33, Chap 1]) and

$$T(\theta_i, \theta_r) = 1 - R(\theta_i, \theta_r). \quad (10)$$

The resultant optical force exerted by the laser is obtained by integrating (6) over all the surface of particle which is effectively illuminated by the beam (the region in which  $\hat{k}_0 \cdot (-\hat{n}^0) \geq 0$ ). To do so, we need to know the power density carried by each ray. In this work, we suppose that the electric field is given by  $\vec{E}(\rho, z) \propto \Psi(\rho, z) \hat{x}$ , in which  $\Psi(\rho, z)$  is given by (3). Therefore, the power density  $P_i$  is:

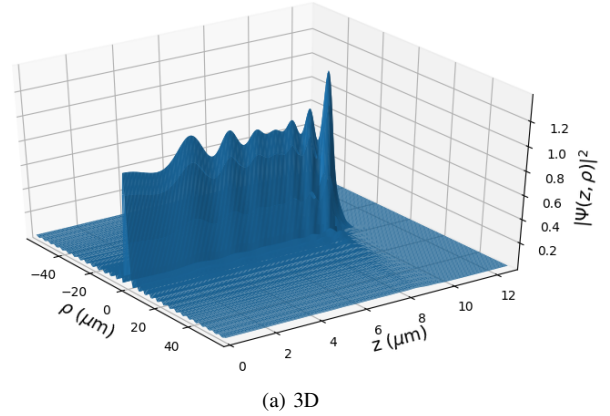
$$dP_i = \vec{S} \cdot d\vec{A} = |\vec{S}| \cos \theta_i dA \propto |\vec{E}|^2 \cos \theta_i \sin \theta d\theta d\phi, \quad (11)$$

in which  $\vec{S}$  is the Poynting vector and  $\theta$  and  $\phi$  are azimuthal and polar angles of the spherical coordinates. From now on, we shall consider only normalized fields, which means that the intensity of a corresponding ideal BB is taken as being unitary.

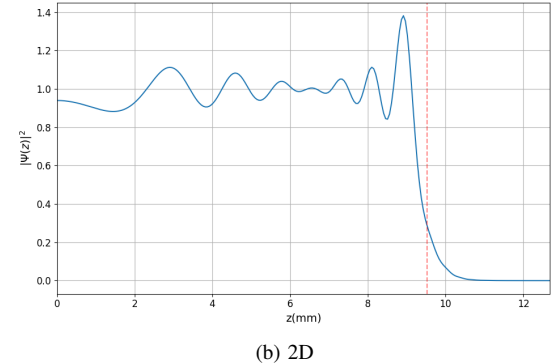
### III. RESULTS

To perform the numerical analysis of optical forces exerted on dielectric particles, we define a TBB with vacuum wavelength  $\lambda_0 = 1064$  nm, aperture radius  $R = 1$  mm,  $L = 3R^2$ ,  $q_r = 6/L$ , axicon angle  $\theta_a = 6^\circ$ ,  $q = 0$  and  $N = 21$  (thus, we have  $2N + 1 = 43$  different BGBs). These conditions lead to  $Z_{max} = 9.51$  mm. We also supposed that the electric field of our TBB is linearly polarized in  $\hat{x}$ , that is,  $\vec{E}(\rho, z) = \Psi(\rho, z) \hat{x}$ , in which  $\Psi(\rho, z)$  is given by (3). The intensity of our corresponding TBB can be seen in Fig. 2.

In our first analysis, we suppose that the TBB impinges on a spherical dielectric particle with radius  $R_p = 18 \mu\text{m}$ . The longitudinal force exerted on this scatterer is sketched in Fig. 3 for three relative (to water) refractive indices ( $n_{rel} = 0.95$ , 1.01, and 1.20). Fig. 3 shows that the slopes resemble with the TBB slope in  $\rho = 0$ , whose typical oscillations along  $+z$  are closer of those observed experimentally, in contrast with the ideal case, in which the force magnitude does not change over the propagation. This result was expected for a



(a) 3D



(b) 2D

Fig. 2: TBB with vacuum wavelength  $\lambda_0 = 1064$  nm, medium refractive index  $n_m = 1.33$ , aperture radius  $R = 1$  mm,  $L = 3R^2$ ,  $q_r = 6/L$ , axicon angle  $\theta_a = 6^\circ$ , constant  $q = 0$  and  $N = 21$ .

real BB because of the scatter force's predominance as long as the axicon angle is small, which implies in a TBB with an extended focus.

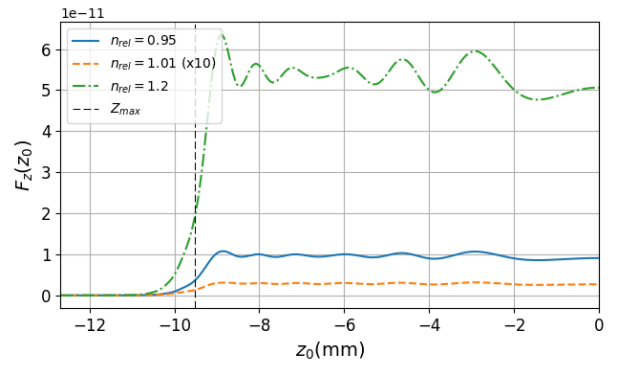
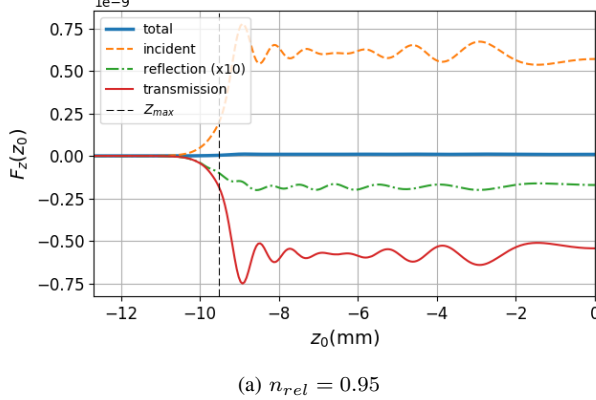


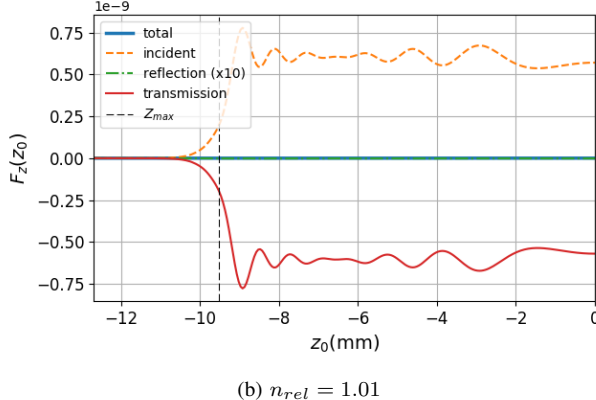
Fig. 3: Longitudinal force for the TBB over a dielectric spherical particle with radius  $R_p = 18 \mu\text{m}$  in function of  $z_0$  with  $x_0 = 0$  and  $y_0 = 0$ . Three different  $n_{rel}$  are shown. For visualization purposes, slope  $n_{rel} = 1.01$  is scaled by 10.

To deepen in our longitudinal force analysis, Fig. 4 shows the contribution of each term of (8) for the same three particles defined before. We call the terms 1,  $R \exp(-i2\theta_i)$  and  $T^2 \exp[-i2(\theta_i - \theta_r)]/[1 + R \exp(i2\theta_r)]$  of (8) as incident, reflection and transmission contribution respectively. We

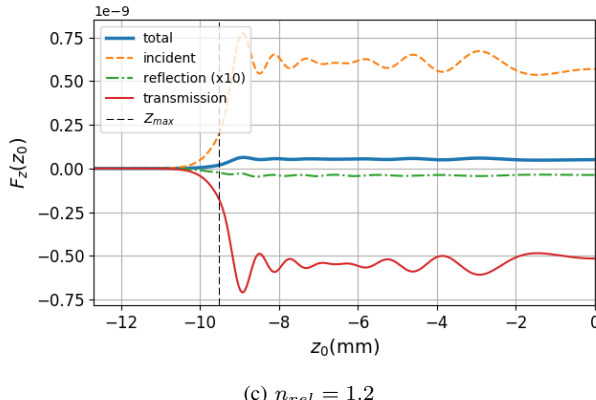
observe, as expected, the incident contribution has the same value for the three beads; the reflection contribution has its magnitude much smaller compared with the other two and transmission has a small variation for each particle. Finally, we can infer that the three terms are proportional to  $|\Psi|^2$ , which leads to the longitudinal force  $F_z$  being proportional to the intensity and, therefore, never cross  $F_z = 0$ .



(a)  $n_{rel} = 0.95$



(b)  $n_{rel} = 1.01$



(c)  $n_{rel} = 1.2$

Fig. 4: Decomposition of the longitudinal force for the TBB over a dielectric spherical particle with radius  $R_p = 18 \mu\text{m}$  in function of  $z_0$  with  $x_0 = 0$  and  $y_0 = 0$ . Three different  $n_{rel}$  are shown: (a) for  $n_{rel} = 0.95$ , (b) for  $n_{rel} = 1.01$  and (c) for  $n_{rel} = 1.2$ . For visualization purposes, reflection slope is scaled by factor of 10.

The longitudinal force when the beam aperture is fixed at  $z_0 = -Z_{max}$  and moved along  $x$  axis is shown in Fig. 5, for

the particle defined before. As we can see, there is not a point of stable equilibrium when the aperture is moving transversely. It is worth to point that longitudinal forces reaches a maximum value when  $x_0 = \pm R_p$ .

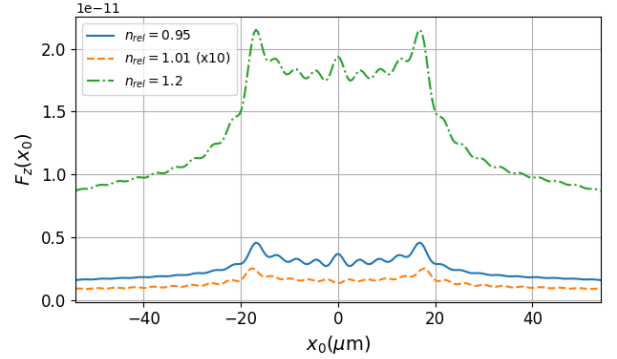


Fig. 5: Longitudinal force for the TBB over a dielectric spherical particle with radius  $R_p = 18 \mu\text{m}$  in function of  $x_0$  with  $y_0 = 0$  and  $z_0 = 0$ . Three different  $n_{rel}$  are shown. For visualization purposes, slope  $n_{rel} = 1.01$  is scaled by factor of 10.

#### IV. CONCLUSION

For the small axicon angles adopted in our analysis, points of stable equilibrium along  $+z$  did not occur, as expected. To observe such points, it is imperative to increase the axicon angle, thus forcing us to abandon the paraxial regime altogether. But doing that involves dealing with full vector beams. Since the original method deals exclusively with scalar beams, such a situation turns out to be out of the scope of the present work. It can and must, however, be considered elsewhere.

From this first attempt towards the incorporation of TBBs in optical force calculations under the ray optics regime, we can see clearly that it is possible to extend this analysis to others truncated beams like TGBs and TBGBs. Furthermore, one must also consider the behavior of the transverse forces, and the consequences of introducing losses. This is currently in progress.

#### REFERENCES

- [1] A. Ashkin, "Atomic-beam deflection by resonance-radiation pressure," *Physical Review Letters*, vol. 25, no. 19, p. 1321, 1970.
- [2] —, "Acceleration and trapping of particles by radiation pressure," *Physical review letters*, vol. 24, no. 4, p. 156, 1970.
- [3] —, "History of optical trapping and manipulation of small-neutral particle, atoms, and molecules," *Selected Topics in Quantum Electronics, IEEE Journal of*, vol. 6, no. 6, pp. 841–856, 2000.
- [4] A. Ashkin and J. Dziedzic, "Optical levitation by radiation pressure," *Applied Physics Letters*, vol. 19, no. 8, pp. 283–285, 1971.
- [5] —, "Optical levitation of liquid drops by radiation pressure," *Science*, vol. 187, no. 4181, pp. 1073–1075, 1975.
- [6] A. Ashkin, J. Dziedzic, J. Bjorkholm, and S. Chu, "Observation of a single-beam gradient force optical trap for dielectric particles," *Optics letters*, vol. 11, no. 5, pp. 288–290, 1986.
- [7] A. Ashkin and J. Dziedzic, "Optical trapping and manipulation of viruses and bacteria," *Science*, vol. 235, no. 4795, pp. 1517–1520, 1987.
- [8] A. Ashkin, J. Dziedzic, and T. Yamane, "Optical trapping and manipulation of single cells using infrared laser beams," *Nature*, vol. 330, no. 6150, pp. 769–771, 1987.

- [9] A. Ashkin, "Forces of a single-beam gradient laser trap on a dielectric sphere in the ray optics regime," *Biophysical journal*, vol. 61, no. 2, p. 569, 1992.
- [10] —, "Optical trapping and manipulation of neutral particles using lasers," *Proceedings of the National Academy of Sciences*, vol. 94, no. 10, pp. 4853–4860, 1997.
- [11] R. W. Steubing, S. Cheng, W. H. Wright, Y. Numajiri, and M. W. Berns, "Laser induced cell fusion in combination with optical tweezers: the laser cell fusion trap," *Cytometry*, vol. 12, no. 6, pp. 505–510, 1991.
- [12] V. Emiliani, D. Cojoc, E. Ferrari, V. Garbin, C. Durieux, M. Coppey-Moisan, and E. Di Fabrizio, "Wave front engineering for microscopy of living cells," *Optics Express*, vol. 13, no. 5, pp. 1395–1405, 2005.
- [13] M. W. Berns, W. H. Wright, B. J. Tromberg, G. A. Profeta, J. J. Andrews, and R. J. Walter, "Use of a laser-induced optical force trap to study chromosome movement on the mitotic spindle," *Proceedings of the National Academy of Sciences*, vol. 86, no. 12, pp. 4539–4543, 1989.
- [14] M. Waleed, S.-U. Hwang, J.-D. Kim, I. Shabbir, S.-M. Shin, and Y.-G. Lee, "Single-cell optoporation and transfection using femtosecond laser and optical tweezers," *Biomedical optics express*, vol. 4, no. 9, pp. 1533–1547, 2013.
- [15] G. Wright, M. J. Tucker, P. C. Morton, C. L. Sweitzer-Yoder, and S. E. Smith, "Micromanipulation in assisted reproduction: A review of current technology," *Current Opinion in Obstetrics and Gynecology*, vol. 10, no. 3, pp. 221–226, 1998.
- [16] J. C. Crocker and D. G. Grier, "Microscopic measurement of the pair interaction potential of charge-stabilized colloid," *Physical review letters*, vol. 73, no. 2, p. 352, 1994.
- [17] D. G. Grier, "Optical tweezers in colloid and interface science," *Current opinion in colloid & interface science*, vol. 2, no. 3, pp. 264–270, 1997.
- [18] O. Kučera, D. Havelka, and M. Cifra, "Vibrations of microtubules: Physics that has not met biology yet," *Wave Motion*, 2016.
- [19] G. Wang, E. M. Sevick, E. Mittag, D. J. Searles, and D. J. Evans, "Experimental demonstration of violations of the second law of thermodynamics for small systems and short time scales," *Physical Review Letters*, vol. 89, no. 5, p. 050601, 2002.
- [20] L. A. Ambrosio and H. E. Hernández-Figueroa, "Integral localized approximation description of ordinary bessel beams and application to optical trapping forces," *Biomedical optics express*, vol. 2, no. 7, pp. 1893–1906, 2011.
- [21] —, "Gradient forces on double-negative particles in optical tweezers using bessel beams in the ray optics regime," *Optics express*, vol. 18, no. 23, pp. 24 287–24 292, 2010.
- [22] —, "Radiation pressure cross sections and optical forces over negative refractive index spherical particles by ordinary bessel beams," *Applied optics*, vol. 50, no. 22, pp. 4489–4498, 2011.
- [23] J. Durnin, J. Miceli Jr, and J. Eberly, "Diffraction-free beams," *Physical Review Letters*, vol. 58, no. 15, p. 1499, 1987.
- [24] J. Durnin, "Exact solutions for nondiffracting beams. i. the scalar theory," *JOSA A*, vol. 4, no. 4, pp. 651–654, 1987.
- [25] J. Goodman, "Introduction to fourier optics," 2008.
- [26] M. Zamboni-Rached, E. Recami, and M. Balmi, "Simple and effective method for the analytic description of important optical beams when truncated by finite apertures," *Applied optics*, vol. 51, no. 16, pp. 3370–3379, 2012.
- [27] P. P. J. S. Arantes and L. A. Ambrosio, "Cálculo de forças ópticas no regime de rayleigh usando soluções analíticas para feixes de bessel escalares e truncados," *MOMAG*, 2016.
- [28] F. Gori, G. Guattari, and C. Padovani, "Bessel-gauss beams," *Optics communications*, vol. 64, no. 6, pp. 491–495, 1987.
- [29] J. H. Poynting, "On the transfer of energy in the electromagnetic field," *Philosophical Transactions of the Royal Society of London*, vol. 175, pp. 343–361, 1884.
- [30] G. Roosen, "La levitation optique de sphères," *Canadian Journal of Physics*, vol. 57, no. 9, pp. 1260–1279, 1979.
- [31] M. Rocha, "Optical tweezers for undergraduates: theoretical analysis and experiments," *American Journal of Physics*, vol. 77, no. 8, pp. 704–712, 2009.
- [32] Y. Zhang, Y. Li, J. Qi, G. Cui, H. Liu, J. Chen, L. Zhao, J. Xu, and Q. Sun, "Influence of absorption on optical trapping force of spherical particles in a focused gaussian beam," *Journal of Optics A: Pure and Applied Optics*, vol. 10, no. 8, p. 085001, 2008.
- [33] M. Born and E. Wolf, *Principles of optics: electromagnetic theory of propagation, interference and diffraction of light*. CUP Archive, 2000.